Characterization and Modeling of Engineering Friction and Wear with LS-DYNA

S. Dong[1], A. Sheldon[2]

[1]The Ohio State University
[2]Honda R&D Americas, Inc.

In mechanical systems, friction and wear usually take place concurrently between two surfaces when they slide or roll relative to each other. Friction exhibits resistance to the relative motion which may vary with different normal loads and relative velocities, while wear is the removal and displacement of the materials from one or both surfaces. The initiation of significant surface wear, in turn, changes the friction, and therefore the overall contact properties. This occurs more often when there are differences in hardness and/or surface roughness between the two surfaces. This paper presents experimental characterization of friction and surface wear between different material combinations. Materials tested, from hard to soft, include coated steel, plastics, ATD rubber, and roof linear fabric. Static and dynamic friction coefficients are measured using a pin-on-disc tribometer under various normal loads and linear velocities. It was found that the friction coefficient decreases when surface wear first takes place. The modeling of friction and wear is then implemented in LS-DYNA. The relationship between friction coefficients, normal stress, and linear velocity is defined in *CONTACT and the wear properties are defined in *CONTACT_ADD_WEAR. Friction can play different roles in different models. It was found that in models where large relative motion is present friction can play an important role. Parametric studies were performed to investigate the influence of wear and friction properties in crash models.

1 Introduction

In mechanical systems, friction and wear usually take place concurrently between two surfaces when they slide or roll relative to each other. Friction causes resistance to the relative motion which may vary with different normal loads and relative velocities, while wear is the removal and displacement of the materials from one or both surfaces (Bhushan, 2002). Friction and wear can be reduced by using traditional lubrication methods such as grease or oil. In addition, ultrasonic vibrations can also be used to reduce friction, wear, and stick-slip at an interface (Dong & Dapino, 2014). The accurate modeling of friction in computer-aided engineering (CAE) can enhance the accuracy and quality of a model. However, the accurate simulation of friction in finite element (FE) models has not received significant attention. In LS-DYNA, the cards in *CONTACT provides options to assign static and dynamic friction coefficients (Fig.1). By changing the parameters, one can also define relationships between coefficients of friction and velocity under different pressure loads.

Card 2	1	2	3	4	5	6	7	8
Variable	FS	FD	DC	VC	VDC	PENCHK	BT	DT
Type	F	F	F	F	F	I	F	F
Default	0.	0.	0.	0.	0.	0	0.	1.0E20
Remarks								

*Fig.1: Friction card in *CONTACT in LS-DYNA.*

However, often in FE models, friction is represented by a few approximated coefficient of frictions (CoF) values, despite the wide range in material and geometry between parts that may come into contact. It is critical in some cases to use the correct friction coefficients while in others it is less essential. This paper firstly reports experimental work for determining the correct friction coefficients under different normal stresses and linear velocities for certain materials combinations. Then, different

© 2017 Copyright by DYNAmore GmbH

models are used to demonstrate both the cases where friction is critical to be characterized and others where it is not.

2 Experimental set-up

A pin-on-disc tribometer is employed to measure friction forces between different materials. The set-up of the tribometer is shown in Fig.2. The concept is to measure the friction between a stationary pin and a rotating disc using a load cell. Schematics of the set-up are shown in Fig.3. The test sample is placed and fixed on a platform which is rotated by a DC motor. The pin is held by a gymbal assembly which allows different normal loads applied at the interface by adding different weights. The friction force at the interface is measured by a load cell.

All friction tests follow the procedures as below:

1. Place the pin on the disc surface, put on the weight for the normal loading and load cell balancing.
2. Start data acquisition.
3. Turn the control knob of the motor slowly until there is slip motion between the pin and disc.
4. Continue increasing the speed of the motor until it reaches the limit.
5. Turn off the motor and the data acquisition.

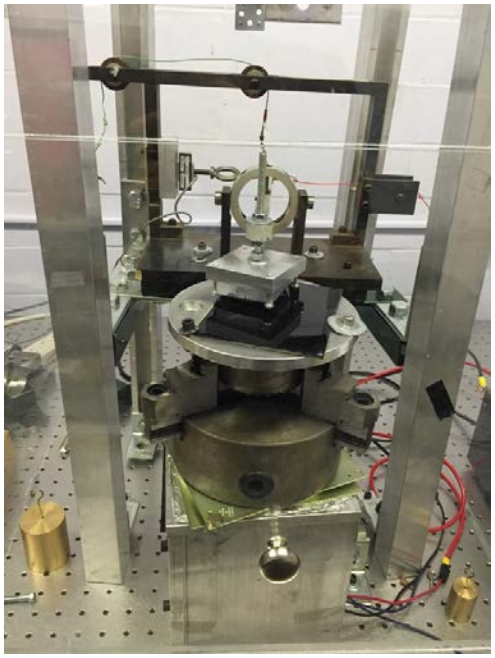

Fig.2: Experimental Set-up for measuring engineering friction.

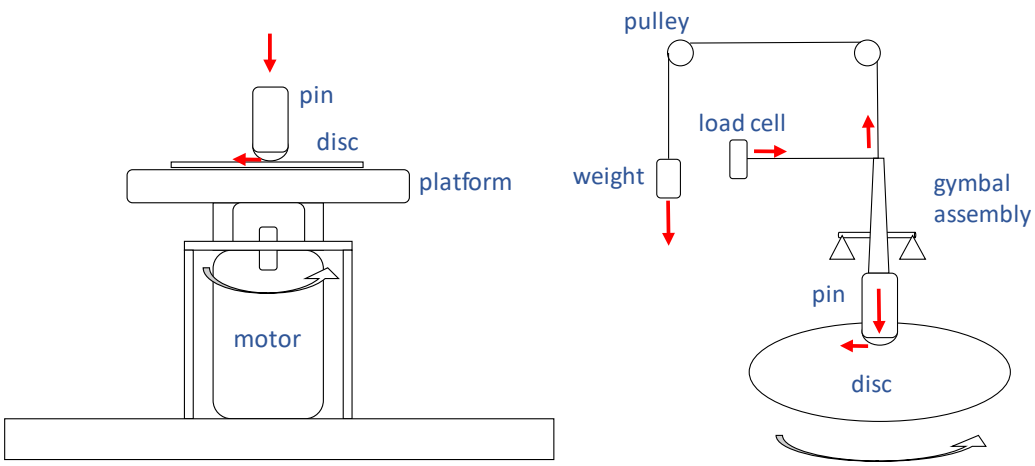

© 2017 Copyright by DYNAmore GmbH

(a) (b)

Fig.3: Schematics of the experimental set-up: (a) bottom part; (b) gymbal assembly.

Groups of friction tests have been conducted in this project, the conditions of which are listed in Table 1. Test group 1 is conducted between a pedestrian rubber piece and steel plate used for the hood of a vehicle. This material combination is picked in order to better simulate the impact between the pedestrian headform and the hood. Textbook values could be employed by these models, but they have shown some discrepancies in the simulation results that were not solved otherwise, especially in the magnitude of the acceleration at the first peak when the impact initiates. The material is pedestrian headform rubber against Class A steel. In vehicles, Class A steel parts are the ones that have been painted and treated with a layer of clear coating for aesthetic purposes. The linear speed is adjusted by changing the diameter of rotation and the rotational speed. Part of the details of this study have been published by Dong et. al. previously (Dong et. al. 2016).

Parameter	**Test Groups**		
	1	**2**	**3**
Pin material	PED Rubber	ATD Rubber	ATD Rubber
Disc material	Class A coated steel	Roof liner	Plastics
Linear speed (mm/s)	0-1500		
Normal load (N)	4 – 17		
Nominal diameter of rotation (mm)	36		
Sampling frequency (Hz)	400		

Table 1: Experimental parameters of the sample tests.

3 Experimental results

An example of a single test is shown in Fig.4. The test lasts for approximately 25 seconds. From 10 to 20 s, motor was turned on and relative motion between pin and disc is created, thus the readings of friction shown in the curve. The friction measurement has fluctuations due to the fact that the disc is not perfectly perpendicular to the pin and therefore small amount of runout creates variation of normal forces and thus friction forces measured. The average and standard deviation of the measurement were calculated. The coefficient of friction under this condition is obtained accordingly.

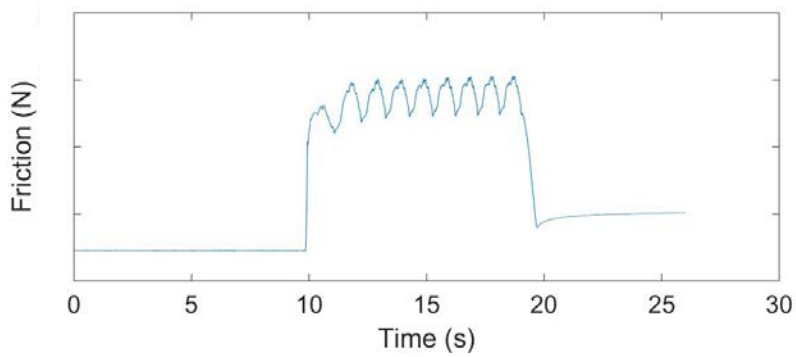

Fig.4: Time dependent recording of one friction measurement.

Following the same procedure, all the tests under different normal loads and linear velocities are conducted. Figure 5 shows the measurements of friction forces and the normalized friction coefficients under all conditions. Each marker represents one test. The normalized friction coefficient between rubber and a class A steel plate is approximately 0.8. This result is much higher than what the textbook values indicate. It remains virtually constant as the linear velocity increases. Also, between different levels of normal stresses, the friction coefficient remains virtually constant. It is the clear coating that creates a strong sticking force between the rubber piece and the steel plates, which results in much larger friction forces under the same normal loads.

© 2017 Copyright by DYNAmore GmbH

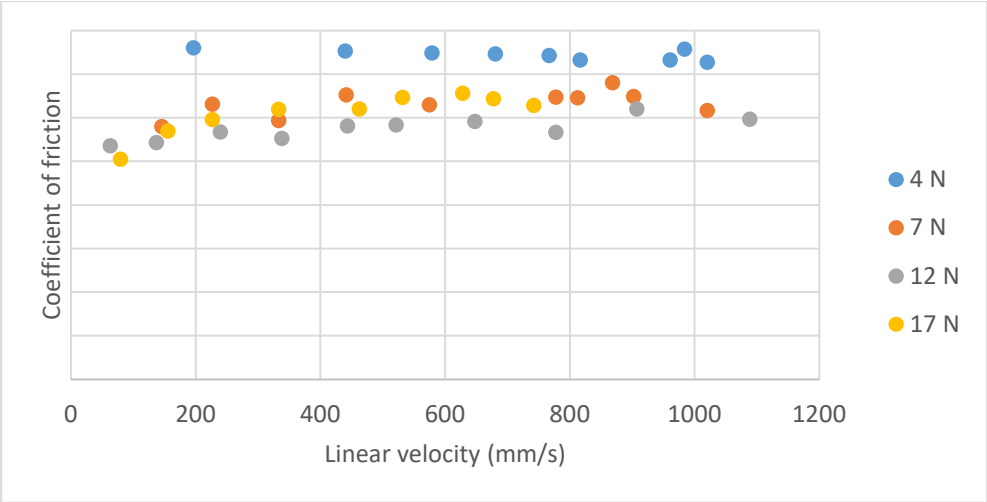

Fig.5: Calculated coefficient of friction between rubber and class A coated steel.

More material combinations are tested, including ATD rubber on plastic fascia as well as ATD rubber on roof liner. Here, an example between rubber and roof liner is shown to demonstrate the frictional characteristic between two relatively soft materials.

The experimental set-up is shown in Fig.6. It is the same set-up in principle but with modifications to adapt the material specimens. ATD rubber is inserted into an aluminium holder and stays stationary during the tests, while a flat piece of roof liner materials is cut out, fixed on the platform, and rotated at different speeds.

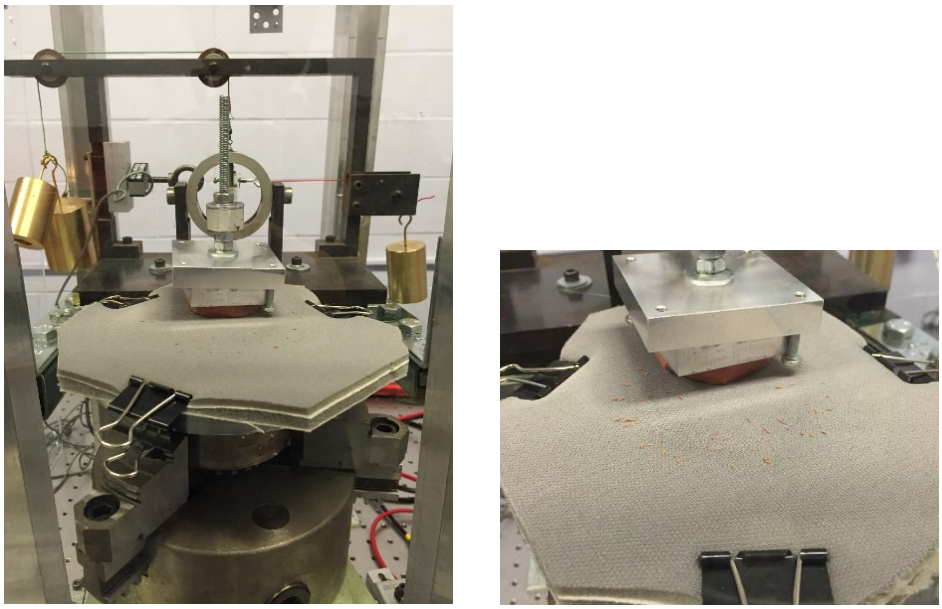

Fig.6: Experimental set-up for ATD rubber vs. roof liner.

Four testing groups are shown in this case: 4, 7, 12, and 17 N. During the test for each normal load, a range of linear velocities are tested approximately from 0 to 1500 mm/s. Due to the soft nature of both materials, the contact area between the two pieces increases significantly as the normal load increases, which results in different friction coefficient between different load groups (Fig.7).

© 2017 Copyright by DYNAmore GmbH

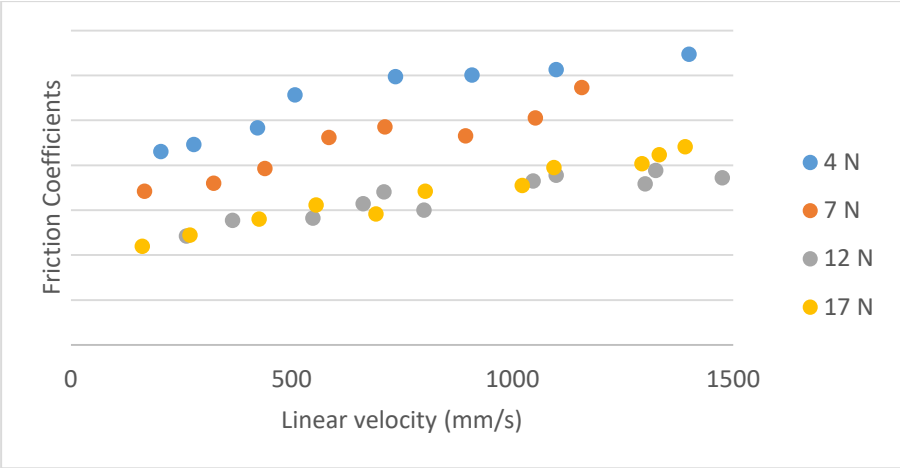

Fig.7: Coefficients of friction under different loads between ATD rubber and roof liner material.

Four testing groups are shown in this case: 4, 7, 12, and 17 N. During the test for each normal load, a range of linear velocities are tested from approximately 0 to 1500 mm/s. Due to the soft nature of both materials, the contact area between the two pieces increases significantly as the normal load increases, which results in different friction coefficient between different load groups.

The results for each load tested are shown in Fig.8. As the linear speed increases, the wear between the rubber and the roof liner initiates, especially on the rubber side. The rubber wear debris can be seen in Fig.6 (b). The reason is that the textile on the surface of the roof linear is rough against the rubber piece despite the soft foam underneath the surface. Similar wear has been observed in the tests between ATD rubber against a plastic fascia due to the patterns on the surface of the fascia.

Wear is caused by the frictional heat generated during the sliding. The higher the normal load and linear velocity are, the higher the friction heat is. For higher normal loads, the linear velocity at which the wear initiates is lower. For example, for the 4 N case, wear starts to appear at 850 mm/s, while for 17 N, wear initiates at 550 mm/s.

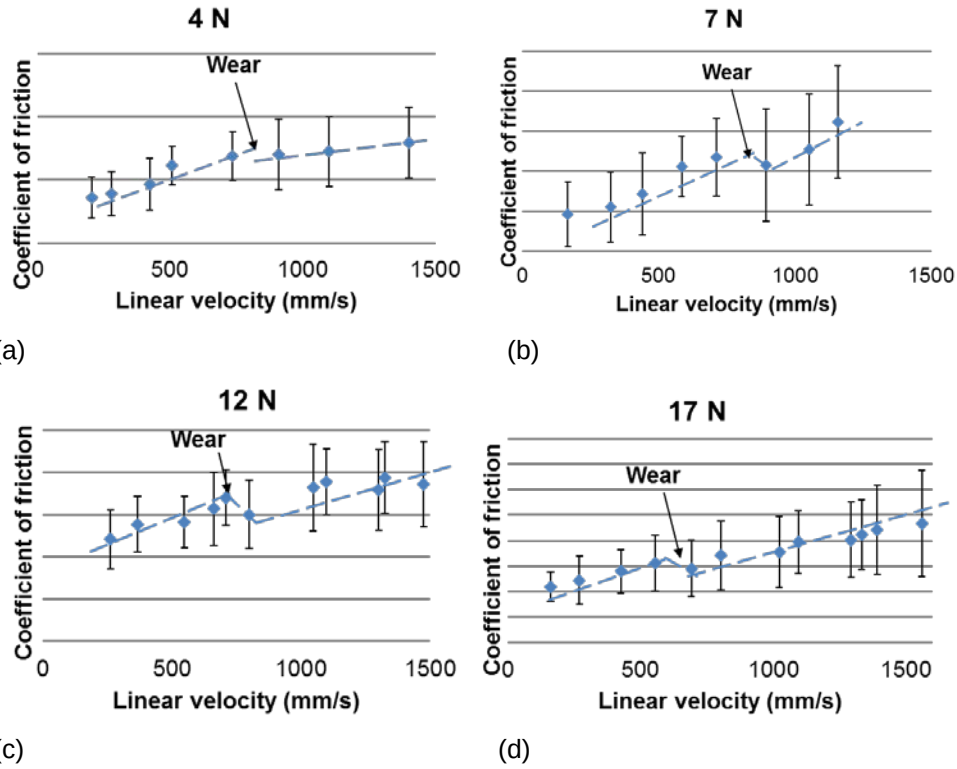

Fig.8: Coefficients of friction under individual load between ATD rubber and roof liner material.

© 2017 Copyright by DYNAmore GmbH

The friction coefficient has a sudden decrease when wear takes place for all four load cases. This occurs because the wear debris gets trapped in between the two surfaces that were originally in contact. The wear debris acts as third-body lubricants in this case. The original contact between the two opposite surfaces is reduced by the lubricants. Also part of the original sliding is transformed into rolling friction, which is intrinsically smaller than sliding friction. This lubrication effect becomes more evident when the two contacting materials are harder.

A third test was conducted between ATD rubber and plastics. Similar wear was observed in the tests, as shown in Fig.9. The pattern on the surface of the plastic plate increased the roughness and therefore the surface wear of the rubber piece.

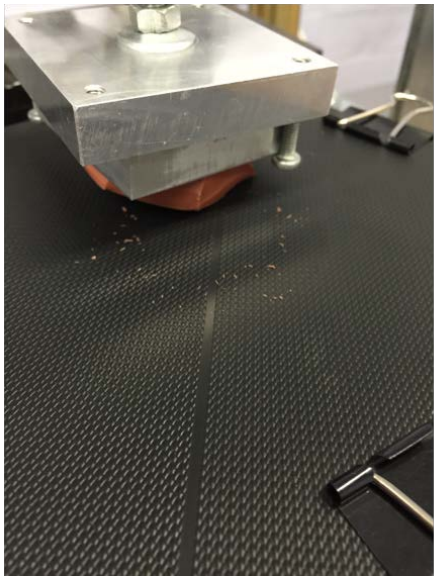

Fig.9: Experimental set-up for ATD rubber vs. plastics.

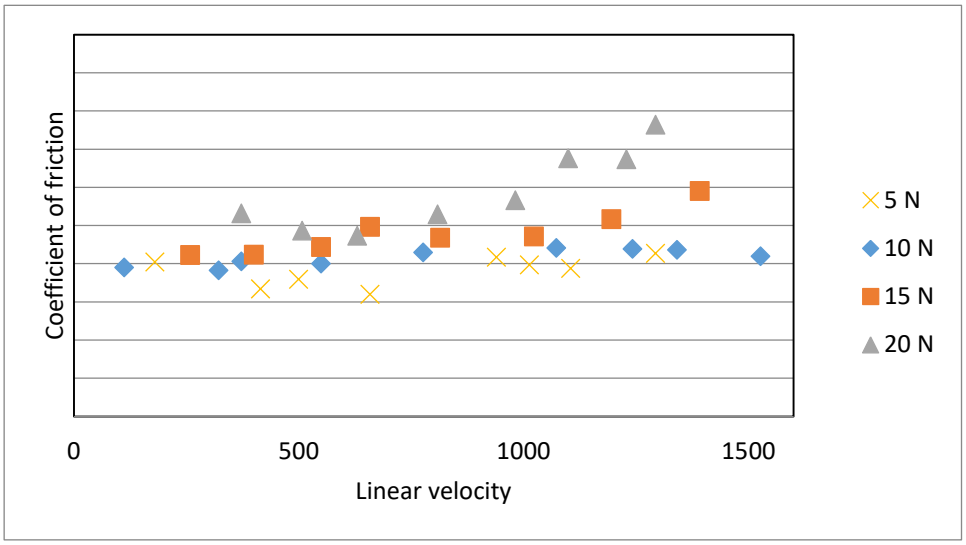

Fig.10: Testing results between ATD rubber and plastics.

© 2017 Copyright by DYNAmore GmbH

4 Simulation models

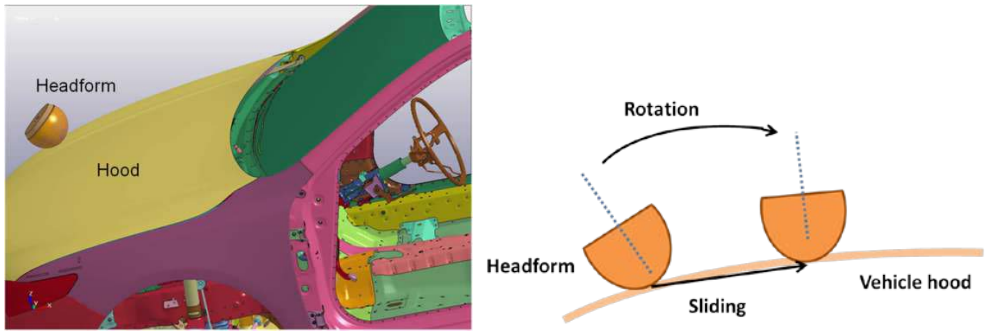

Fig.11: Schematics of the impact interaction between the headform and a hood.

The measured coefficient of friction could enhance the match between the test and simulation in the pedestrian-to-hood impact model shown in Fig.11. The headform hits the hood and then slides and rotates along the length of the hood. Two indices are employed to evaluate the influence of the coefficient of friction on crash model accuracy: the peak value of the acceleration and the head injury criterion (HIC) value.

The time-dependent acceleration curves are shown in Fig.12. The red curve shows the simulation with the textbook values of friction coefficient. This has discrepancies from the measured curve in blue, especially the first peak value when the impact takes place. A new simulation with the measured friction coefficient is conducted and compared with the test data and the simulation with textbook friction coefficients. The simulation with the measured friction coefficient is able to match the magnitude of the acceleration peak, and improve the HIC (IIHS, 2009) value correlation. It is evident that a higher coefficient (measured) results in higher peak acceleration at impact.

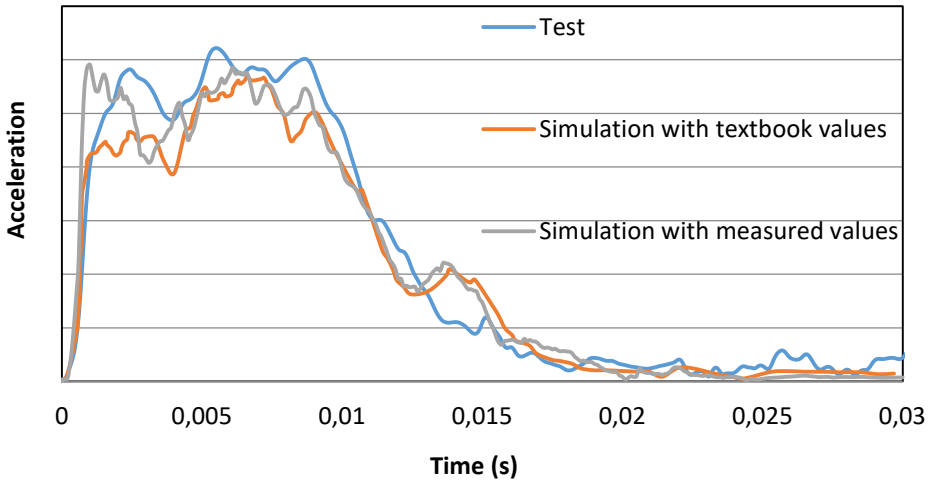

Fig.12: Comparison between simulations and test data.

In order to further investigate the relationship between friction coefficient and peak values of acceleration, a parametric study was conducted and published previously (Dong et al., 2016). The normalized coefficient of friction was set to be 0, 0.02, 0.05, 0.1, 0.2, 0.3, 0.4, 0.5, 0.6, 0.8, 1, 2, respectively for each case.

It was shown that the change of friction coefficient has significant influence in the first peak value of the acceleration curve, which takes place within the first 0.002 s of the impact event. It is evident that the peak values start low when friction coefficient is 0, increase gradually as the coefficient increases, and finally jump to a higher level and reach a steady state as the friction coefficient continues to increase. Two distinct groups can be observed in Fig.13.

© 2017 Copyright by DYNAmore GmbH

The relationship between the peak value of acceleration and the coefficient of friction is plotted in Fig.13. The peak value reaches its steady state when the normalized coefficient of friction is higher than 0.4. The relationship between the HIC value and the normalized coefficient of friction is shown. The value increases when friction coefficient increases. However, the values reach a steady-state when the normalized coefficient is higher than 0.4.

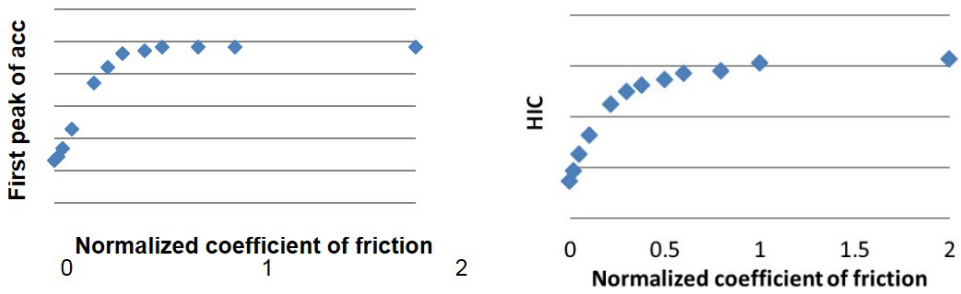

(a) (b)

Fig.13: Relationship between normalized coefficient of friction and (a) peak value; (b) HIC value.

A second crash model that involves the materials tested is a headform hitting the B pillar. The headform hits the seat belt adjuster, the D-ring, and to some degree the pillar garnish which has the same material of the roof liner. In this model, the coefficient of friction measured between the ATD rubber and the plastics as well as the ATD rubber and the roof liner are assigned to replace the textbook values. Figure 14 shows the motion of the headform hitting the pillar. The headform hits straight against the pillar and bounces straight back without obvious sliding or rotation against the pillar.

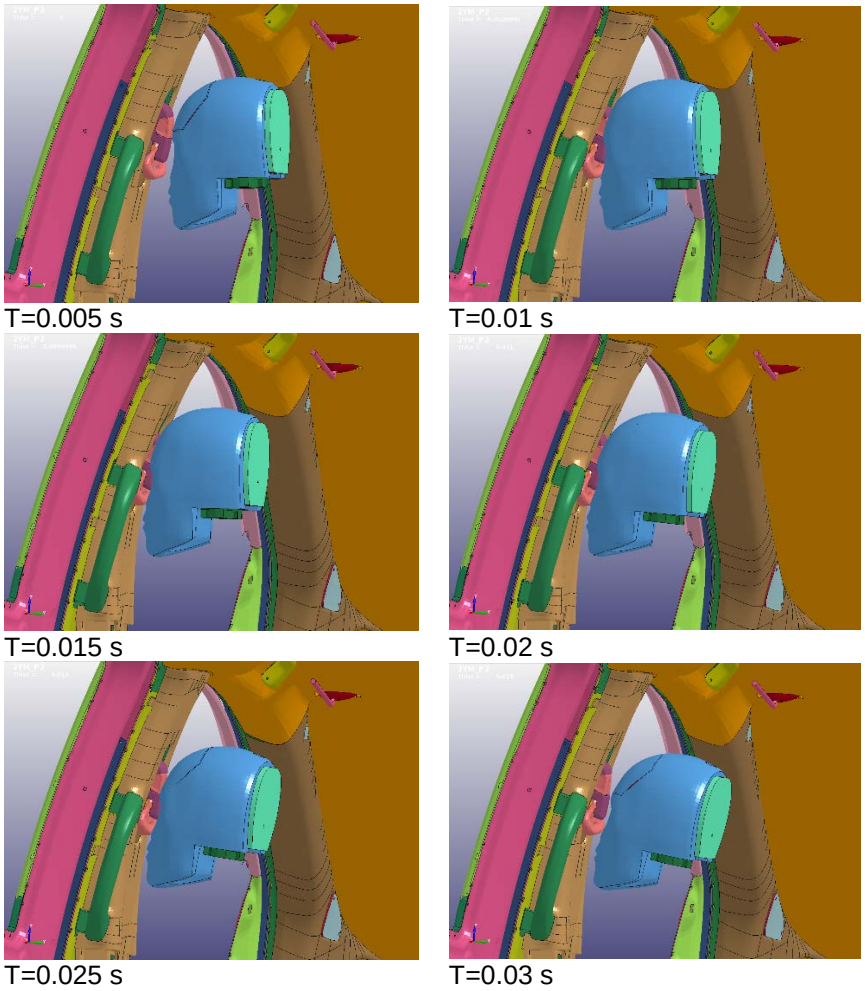

© 2017 Copyright by DYNAmore GmbH

Fig.14: Motion of the headform hitting the side pillar.

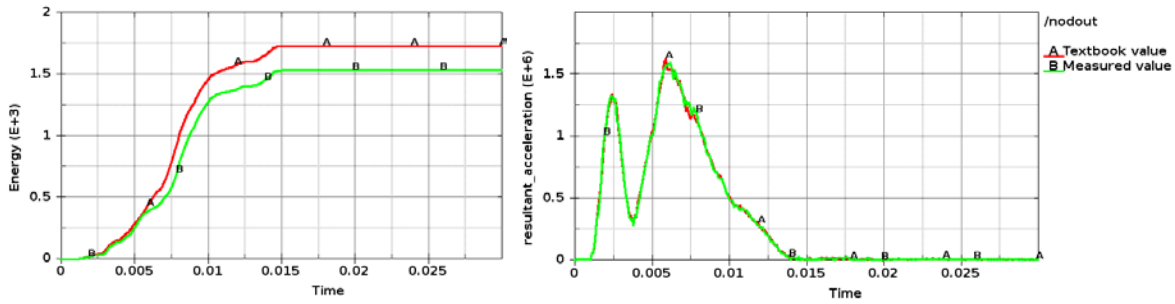

Fig.15: Comparison of the frictional energy and headform acceleration using textbook and measured values.

The frictional energy and deceleration of the headform using both the textbook and measured values are plotted in Fig.15. Due to the difference between the textbook value and the measured value, there exists an evident difference in frictional energy. However, the different friction values result in minimum changes in the headform deceleration. In this case, the friction force is perpendicular to the headfrom motion, thus the influence of the friction on the motion is limited.

A third headform impact simulation is studied where the headform hits the roof liner. In this case, the headform hits and rebounds from a surface that is at an approximately 45 degree angle from the motion direction. Therefore, the friction direction is also at an angle of approximately 45 degree. Thus, friction has some effect on the headform's deceleration, as plotted in Fig.17. There exist discrepancies in both the frictional energy and the peak value of the headfrom deceleration by using textbook versus measured values. The updated peak force provides a better correlation to the test results, which were underestimated by using the textbook values.

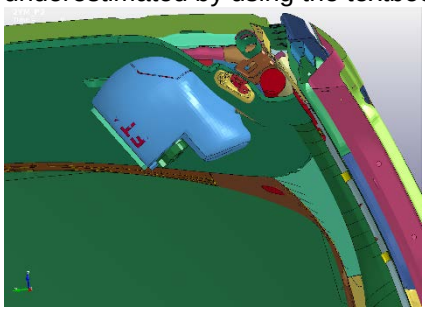

T=0.005 s

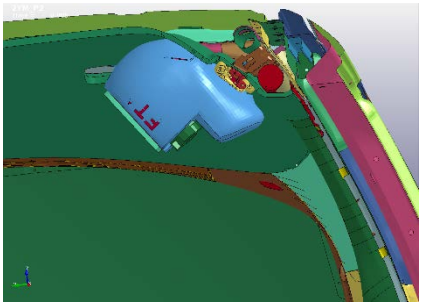

T=0.01 s

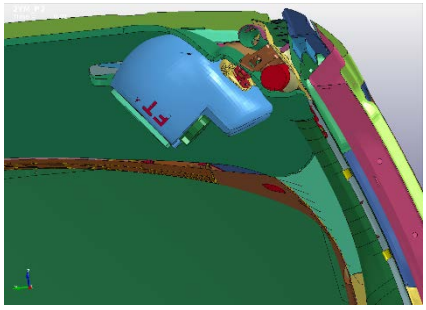

T=0.015 s

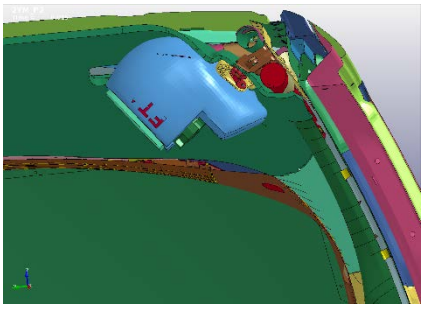

T=0.02 s

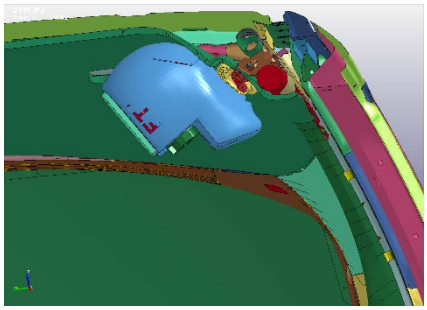

T=0.025 s

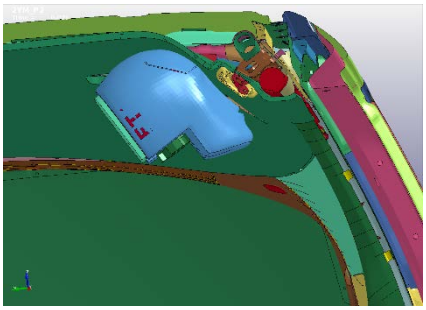

T=0.03 s

© 2017 Copyright by DYNAmore GmbH

Fig.16: Motion of the headform hitting the roof.

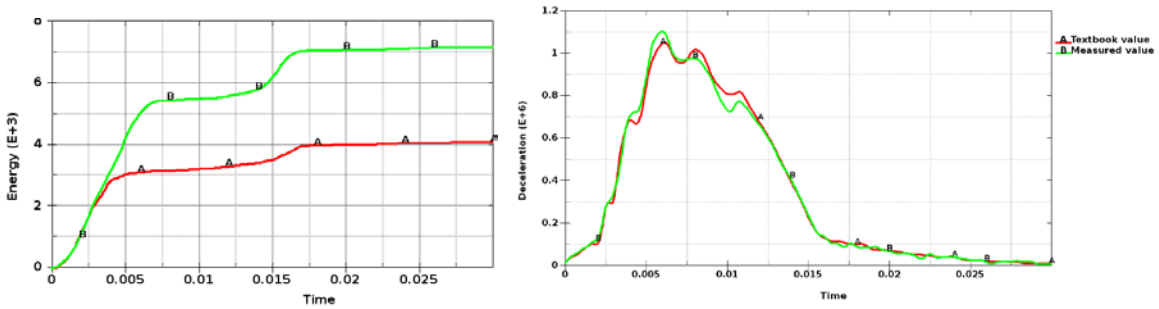

Fig.17: Comparison of the frictional energy and headform acceleration using textbook and measured values.

5 Discussion

In this paper, three crash cases are studied and a hypothesis can be drawn. It is quite common that only the textbook values of friction coefficients are used in crash models and often times they are not accurate to describe the friction properties between different materials. It is desired to have friction coefficients measured for various contacts for different parts. However, given limited resources and means, only the contacts where the surface friction is in line or with an acute angle to the motion should have the priority for testing, especially when there exists large relative displacements. When friction force is almost perpendicular to the direction of motion, it can play a very limited role in the overall motion. Therefore, those cases should have low priorities for testing.

6 Concluding remarks

This paper presents work in characterizing friction and wear properties between materials using the pin-on-disc tribometer. Tests were conducted between pedestrian rubber and coated steel, ATD rubber and roof liner fabric, as well as ATD rubber and plastics. Measured data are then used in pedestrian-hood impact models and driver/passenger headform impact models to enhance the correlation between test and simulation. It is found that friction plays a bigger role when the direction of friction force is in line with the direction of the relative motion while friction has little influence when its direction is perpendicular to the direction of motion.

7 Acknowledgements

The authors would like to thank Honda R&D Americas, Inc. for sponsoring this project and thanks to Kishore Pydimarry and Sameer Gupta for providing testing materials and all their support.

8 References

Bhushan, B., (2002). Introduction to tribology. John Wiley &Sons, New York.

Dong, S. and Dapino, M., (2014). Elastic-plastic cube model for ultrasonic friction reduction via Poisson effect. Ultrasonics, 54, 343-350.

Dong, S. and Dapino, M. (2014). Wear reduction through piezoelectrically-assisted ultrasonic lubrication. Smart Materials and Structures, 23, 104005.

IIHS. (2009). Guidelines for Rating Injury Measures.

Dong, S., Sheldon, A., & Pydimarry, K. (2016). Friction in LS-DYNA®: Experimental Characterization and Modeling Application. 14th International LS-DYNA Users Conference, Detroit, MI, USA.

© 2017 Copyright by DYNAmore GmbH